THE ANATOMICAL RECORD 227:418–426 (1990)

Adaptation of Cancellous Bone to Overloading in the Adult Rat: A Single Photon Absorptiometry and Histomorphometry Study

WEBSTER S.S. JEE AND XIAO JIAN LI
Division of Radiobiology, University of Utah School of Medicine, Salt Lake City, Utah

ABSTRACT Nine-month-old female rats were subjected to right hindlimb immobilization or served as controls for 0, 2, 10, 18, and 26 weeks and were double-labeled with bone markers. The right limb was immobilized against the abdomen and considered unloaded, while the left limb was overloaded during ambulation. Single-photon absorptiometry was performed on intact femur; static and dynamic histomorphometry were performed on 20 μm thick undecalcified frontal sections of the proximal tibial metaphysis. Changes in the continuously overloaded limb was compared to that in both limbs of age-matched control animals.

Single-photon absorptiometry detected increases of bone mineral density of +6%, +6%, and +5% in the proximal and +9%, +7%, and +10% in the distal femoral metaphyses after 10, 18, and 26 weeks of continuous overloading. Morphometrically, significant changes occurred in proximal tibial metaphyses compared to age-matched controls: trabecular area increased +41% and +45%, trabecular number increased +31% and +32%, and trabecular separation decreased −30% and −31% after 18 and 26 weeks of overloading. A significant increase in mineral apposition rate (+38%) was found only at 26 weeks of overloading. Insignificant decreases in both eroded and labeled bone surfaces occurred at all time periods. The histomorphometric changes indicated that increased cancellous bone mass was caused by an increase in bone formation activity (i.e., increases in mineral apposition and bone formation rates) and a decrease in remodeling space (i.e., decrease in bone eroded surface). These findings indicate that the adult skeleton can quickly adapt to the increased biomechanical needs by increasing its cancellous bone mass with an adequate structural pattern. It further support Frost's postulate that increasing skeletal mechanical usage stimulates bone modeling and depresses bone remodeling to increase and maintain bone mass.

Skeletal adaptability or skeletal homeostasis to varying mechanical loads is well established theoretically (Wolff, 1892; Roux, 1895; Frost, 1964, 1973; Martin, 1973; Pauwels, 1980; Currey, 1984; Rubin, 1984; Rubin and Lanyon, 1984; Corwin, 1986). Bone mass increases when the additional mechanical loading is applied in many species including man (See Smith and Gilligan, 1989 for recent comprehensive review). However, no unified concepts regarding the impact of mechanical usage upon the skeleton existed until Frost (1983, 1986a,b, 1987, 1988a,b, in press) proposed that increased mechanical usage stimulates growth and bone modeling and depresses bone remodeling and that decreased mechanical usage depresses growth and bone modeling and stimulates bone remodeling. Increased growth and modeling activities and decreased remodeling increase the bone bank; decreased remodeling activity reduces the remodeling space and the rate of age-related bone loss. Decreased growth and modeling and increased remodeling have the opposite effect. These suggestions were based on clinical and large-animal studies. Whether these postulates hold for the rat skeleton and can be refined form the basis of the current study.

One-legged immobilization by casting seems to be one of the better models to modify mechanical loading because of its ease in application and its reversibility (Mattsson, 1972; Thomaidis and Lindholm, 1976; Sevastikoglou and Mattsson, 1976; Lindgren and Mattsson, 1977; Uhthoff and Jaworski, 1978; Uhthoff et al., 1985). Studies on one-legged immobilization rat model have evaluate the reversibility (Mattsson, 1972; Thomaidis and Lindholm, 1976; Lindgren and Mattsson, 1977) or the hormonal effect (i.e., deficiency of thyroid and parathyroid hormones; Lindgren, 1976a,b) on disuse-induced osteopenia. These studies were mainly focused on the effects of mechanical unloading on bone mass, without proper attention paid to the opposite

Received October 17, 1989; accepted December 5, 1989.

Address reprint requests to Webster S.S. Jee, Ph.D., Building 586, Division of Radiobiology, University of Utah, Salt Lake City, UT 84112.

TABLE 1. Cancellous bone histomorphometry

Measured parameters	Code	Unit	
1. Trabecular area	Tb.Ar	mm^2	
2. Trabecular surface	Tb.Pm	mm	
3. Tissue area	T.Ar	mm^2	
4. Eroded surface	E.Pm	mm	
5. Single labeled surface	sL.Pm	mm	
6. Double labeled surface	dL.Pm	mm	
7. Interlabeling width	Ir.L.Wi	μm	
Derived parameters	**Code**	**Unit**	**Formula**
1. Trabecular area	Tb.Ar	%	Tb.Ar/T.Ar × 100%
2. Trabecular thickness	Tb.Th	μm	(2,000/1.199) × (Tb.Ar/Tb.Pm)
3. Trabecular No.	Tb.N	No./mm	(1.199/2) × (Tb.Pm/T.Ar)
4. Trabecular separation	Tb.Sp	μm	(2,000/1.199) × (T.Ar-Tb.Ar) / Tb.Pm
5. Percent eroded surface	%E.Pm	%	E.Pm/Tb.Pm × 100%
6. Percent labeled surface	%L.Pm	%	(dL.Pm + sL.Pm/2) / Tb.Pm × 100%
7. Mineral apposition rate	MAR	μm/day	Ir.L.Wi/interval
9. Bone formation rate	BFR/Tb.Ar	%/yr	(dL.Pm + sL.Pm/2) × MAR / Tb.Ar × 365 × 100%

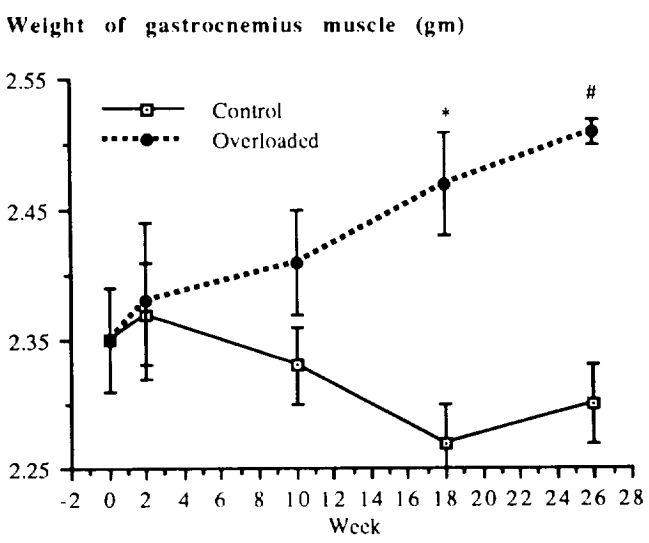

Fig. 1. The time course of the gastrocnemius weight changes in control (□), and overloaded (●) limbs. Y error bar represents standard error. An increase of muscle weight occurred slowly but progressively in the overloaded limb after 2 weeks, resulting in significant differences from age-matched controls by 18 and 26 weeks. *$P < .05$; #$P < .01$.

TABLE 2. Femoral bone mineral density[1] (g/cm^2)

Time	Proximal		Distal	
(weeks)	Control	Overloaded	Control	Overloaded
0	0.309	0.309	0.268	0.268
SD	0.009	0.009	0.008	0.008
2	0.316	0.318	0.268	0.274
SD	0.011	0.009	0.005	0.007
%	102	103	100	102
%-1		101		102
10	0.307	0.327	0.260	0.284
SD	0.014	0.011	0.018	0.014
%	99	106**	97	106**
%-1		106**		109*
18	0.310	0.328	0.262	0.281
SD	0.007	0.009	0.002	0.007
%	100	106**	98	105*
%-1		106**		107**
26	0.312	0.326	0.258	0.285
SD	0.007	0.007	0.012	0.019
%	101	106**	96	106*
%-1		105*		110*
Linear regression analysis (time as independent parameter)				
Intercept	0.31	0.32	0.27	0.27
Slope	0.000	0.001	0.000	0.001
SE	0.000	0.000	0.000	0.000
R	0.04	0.53	0.32	0.44
P	0.8060	0.0047	0.0270	0.0270

[1]% = percent of 0 week control; %-1 = percent of age matched control.
*$P < .05$.
**$P < .01$.

overloaded limb. Thus, very little is known about the skeletal tissue and cellular responses to the impact of the overloading in this one-legged-immobilization model.

The current study is focused on the overloaded limb of the one-legged-immobilized rat. The attempts of relating the changes between muscle weight and cancellous bone mass and characterizing skeletal structural architecture, tissue, and cellular mechanisms in adapting the overloading environment as a function of time were carried out by applying single-photon absorptiometry and selected skeletal histomorphometric analysis. Changes in cancellous bone induced by 2, 10, 18, and 26 weeks of one-legged overloading were characterized and compared to untreated controls (normally ambulating rats).

MATERIALS AND METHODS

Forty-six 9-month-old female virgin Sprague-Dawley rats weighing 310 g were acclimated to local vivarium conditions for 2 weeks. Animals were housed singly in 21 × 32 × 20 cm cages and allowed free access to a pelleted commercial diet (Rodent Chow 5001, Ralston-Purina Co., St. Louis, MO) and deionized water. Six rats were sacrificed as beginning controls (0 week) when the experiment was started. Of the remaining 40 animals, half were one-leg immobilized,

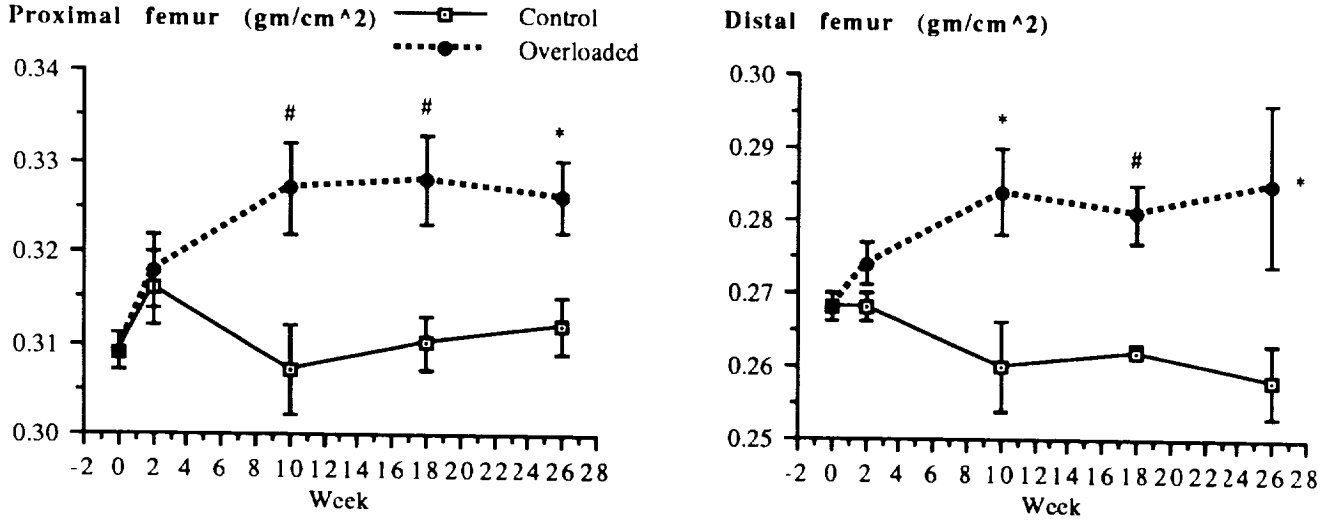

Fig. 2. The time course of the bone mineral density values in the 2 sites of the femur in control (□) and overloaded (●) limbs. Y error bar represents standard error. The proximal and distal femur showed similar changes. The overloaded femur gained bone mineral density, peaking at 10 weeks overloading. *$P < .05$; #$P < .01$.

TABLE 3. Static and dynamic histomorphometry of proximal tibial metaphysis[1]

Time	Trabecular area (mm 2)		Trabecular thickness (μm)		Trabecular No. (#/mm)		Trabecular separation (μm)		Eroded perimeter (%)		Labeled perimeter (%)		Ratio of eroded to label perimeter (Ratio)		Mineral apposition rate (μm/d)		Bone formation rate (%/yr)	
(weeks)	C	OL	C	OL	C	OL	C	OL	C	OL	C	OL	C	OL	C	OL	C	OL
0	1.06	1.06	40.71	40.71	4.35	4.35	189.55	189.55	8.26	8.26	10.65	10.65	0.79	0.79	1.26	1.26	140.79	140.79
SD	0.06	0.06	3.07	3.07	0.23	0.23	10.26	10.26	1.28	1.28	1.94	1.94	0.12	0.12	0.19	0.19	13.00	13.00
2	1.08	1.10	41.02	44.24	4.40	4.15	186.86	197.85	8.24	6.45	10.86	9.08	0.76	0.69	1.20	1.46	110.19	104.4
SD	0.05	0.08	2.63	4.26	0.19	0.34	8.26	16.98	2.25	2.85	2.62	2.21	0.14	0.20	0.23	0.47	31.54	18.6
%	102	104	101	109	101	95	99	104	100	78	102	85	97	88	95	115	78	74***
%-1		102		108		94		106		78		84		91		122		95
10	0.96	1.14	39.71	44.47	3.98	4.25	219.69	192.43	7.70	6.33	9.97	8.64	0.76	0.72	0.83	1.16	84.83	104.36
SD	0.28	0.16	4.78	2.16	0.78	0.40	49.57	24.44	2.51	1.95	1.55	2.04	0.15	0.10	0.31	0.37	16.93	18.57
%	90	107	98	109*	91	98	116*	102	93	77*	94	81	96	92	66**	92	60***	74***
%-1		119		112*		107		88		82		87		96		139		123*
18	0.90	1.26	45.39	48.19	3.31	4.35	258.28	181.70	5.41	4.51	7.18	6.32	0.79	0.69	0.64	0.88	48.08	60.43
SD	0.06	0.27	4.12	9.03	0.29	0.14	23.21	16.14	1.42	2.12	2.46	1.38	0.14	0.18	0.17	0.34	7.62	9.21
%	85**	119*	112*	118*	76***	100	136***	96	65**	55**	67**	59**	100	87	51***	70*	34***	43***
%-1		141**		106		131***		70**		83		88		88		137		126*
26	0.88	1.30	43.49	48.10	3.39	4.49	252.85	174.43	5.73	4.49	7.27	6.16	0.80	0.73	0.57	0.79	43.80	53.70
SD	0.07	0.16	3.23	6.16	0.29	0.08	23.31	6.54	1.78	1.04	2.00	1.57	0.13	0.02	0.07	0.14	7.37	8.35
%	83***	122**	107	118**	78***	103	133***	92*	69*	54**	68**	58**	101	93	45***	63**	31***	38***
%-1		147***		111		132***		69***		78		85		92		138*		123
Linear regression analysis (time as independent parameter)																		
Intercept	1.07	1.06	40.35	41.53	4.40	4.28	187.88	193.73	8.40	7.64	10.95	10.26	0.77	0.74	1.22	1.36	128.05	127.37
Slope	−0.008	0.010	0.140	0.297	−0.045	0.005	2.968	−0.619	−0.116	−0.140	−0.154	−0.177	0.001	−0.001	−0.029	−0.023	−3.758	−3.051
SE	0.002	0.003	0.062	0.108	0.007	0.007	0.458	0.385	0.032	0.046	0.035	0.044	0.002	0.003	0.004	0.008	0.353	0.440
R	0.47	0.58	0.33	0.53	0.69	0.17	0.71	0.34	0.49	0.56	0.56	0.67	0.04	0.08	0.77	0.55	0.85	0.84
P	.0005	.0016	.0240	.0058	.0001	.4450	.0001	.1080	.0003	.0026	.0001	.0001	.7800	.7200	.0001	.0003	.0001	.0001

[1]C = control; OL = overloaded; % = percent of 0 week control; %-1 = percent of age matched control.
*$P < .05$.
**$P < .01$.
***$P < .001$.

and the other half served as normal age-matched controls. Lindgren's method (1976a) was modified to immobilize the animals: the right hindlimb was unloaded by immobilizing it against the abdomen using four layers of elastic bandage tape, with the hip joint in flexion and the knee and ankle joints in extension. Neither the

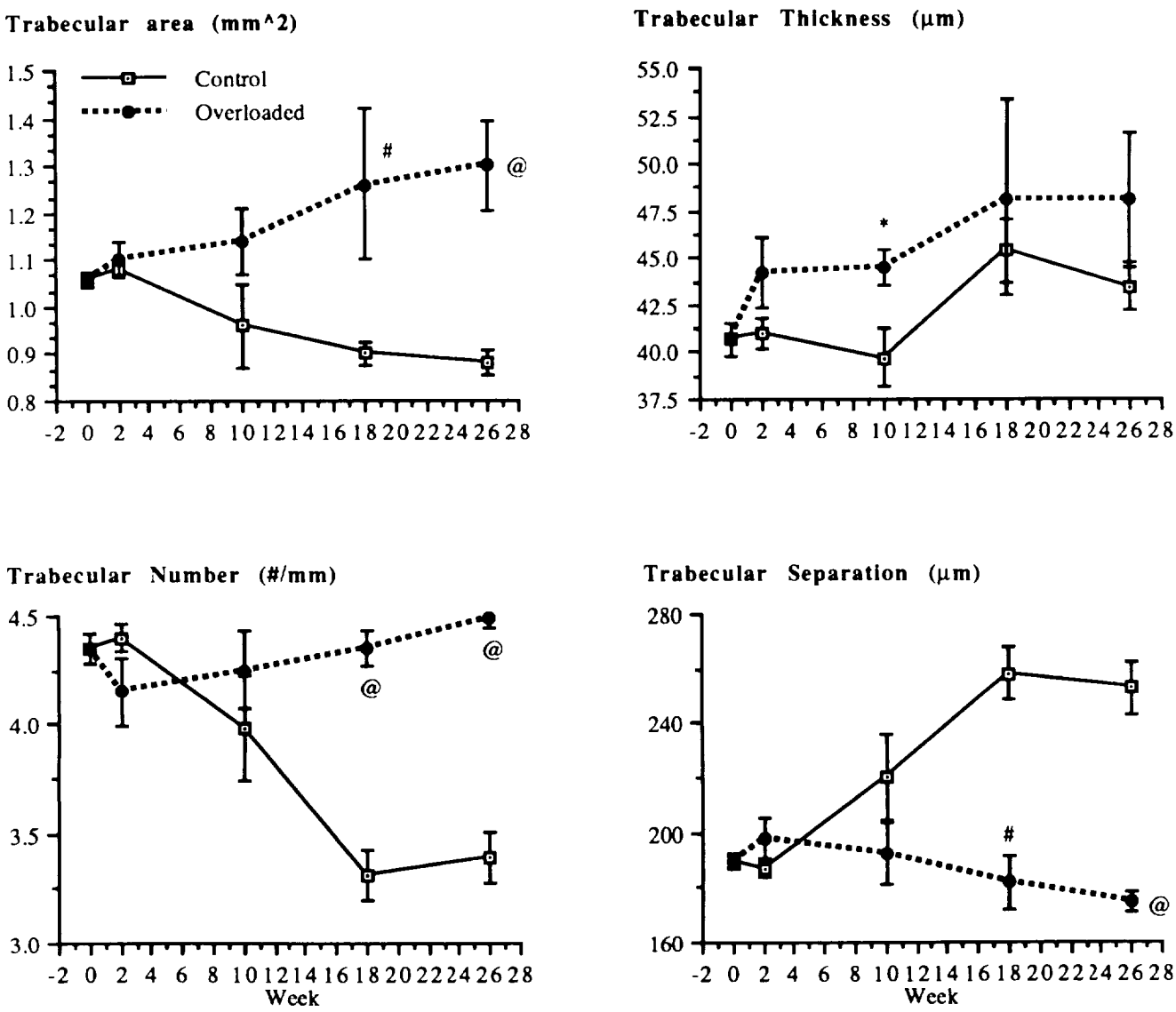

Fig. 3. The time course of static morphometry change of the proximal tibial metaphysis in control (□) and overloaded (●) limbs. Y error bar represents standard error. Increased trabecular area significantly peaked out at 18 weeks with thicker trabeculae. Trabecular number and separation were maintained at basal control levels in the overloaded limb. *$P < .05$; #$P < .01$; @$P < .001$.

right hindlimb nor the applied bandage could touch the cage bottom during the body movement by this method; thus, the left hindlimb was overloaded with the weight normally distributed to 2 hindlimbs. Animals were anesthetized with ether during the taping; the bandage was changed at approximately 2-week intervals. One day after immobilization, rats adapted to the condition and walked or hopped around on three limbs.

Five animals from each group (one-leg immobilization or control) were sacrificed at 2, 10, 18, and 26 weeks during the experiment. All rats were injected subcutaneously with 25 mg/kg of tetracycline-HCl (TC, Lederle Labs, Pearl River, NY) and 10 mg/kg of calcein (CL; Sigma Chemical Co., St. Louis) on 12 and 2 days prior to sacrifice, respectively. All rats were sacrificed by cardiac puncture under ether anesthesia. Gastrocnemius, liver, spleen, lung, adrenal glands, kidneys, and thymus were removed and weighed. Both left and right femora were dissected free of soft tissue for bone mineral content determination. Both left and right tibiae were also dissected, trimmed, and fixed in 70% alcohol for undecalcified bone processing.

Femoral bone mineral content was determined using single-photon absorptiometry (Norland Corporation, Fort Atkinson, WI). Two femoral sites (proximal and distal) were scanned transversely. The proximal site was at the point just distal to the lesser trochanter, and the distal site was at the point just proximal to the femoral condyle. The proximal and distal femoral sites were chosen because they contain a considerable quan-

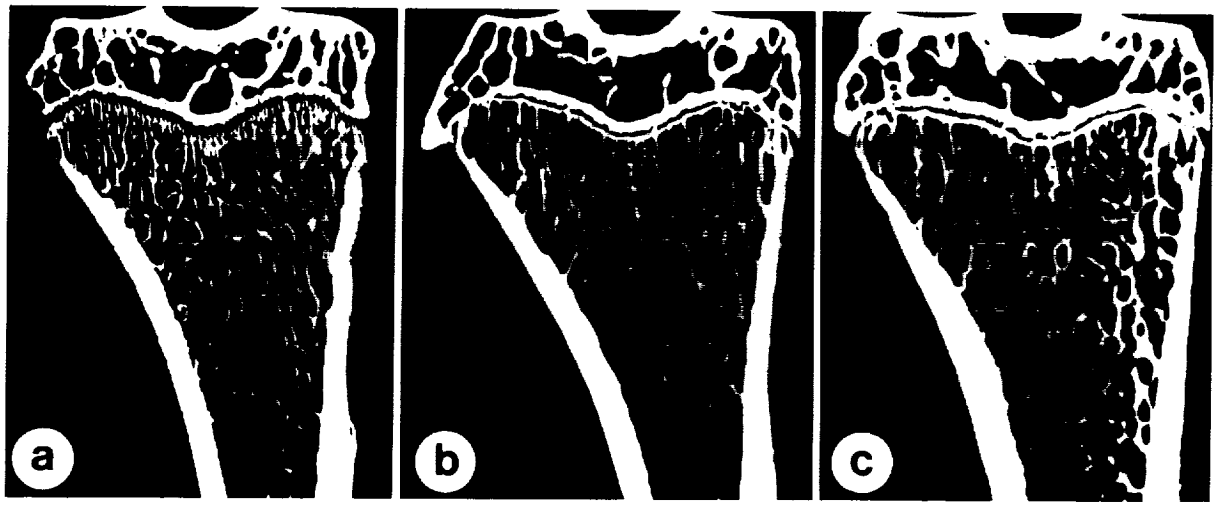

Fig. 4. Microradiographs of proximal tibia from 9-month old basal control (a), 13.5-month old control (b), and 13.5-month old after 18 weeks overloading (c). Fewer and thicker trabeculae are seen in the 13.5 than in 9-month old tibiae (a vs. b). The overloaded tibia conserved the trabecular network structure seen in basal control with more and thicker cancellous bone (c). ×4.

TABLE 4. Percent changes of bone histomorphometry in 26 week overloaded rats and age-matched controls

Parameters	Control vs. 0 wk control	Overloaded Vs. 0 wk control	Overloaded Vs. age control
Trabecular area	−17*	+22*	+47*
Trabecular thickness	+7	+18*	+11
Trabecular No.	−22*	+3	+32*
Trabecular separation	+33*	−8	−31*
Percent eroded surface	−31*	−46*	−22
Percent labeled surface	−32*	−42*	−15
Mineral apposition rate	−55*	−37*	+38*
Bone formation rate	−69*	−62*	+23*

*Significant changes: $P < .05$.

tity of trabecular bone. Bone mineral content (BMC in g/cm) and bone width (BW in cm) were obtained, and bone mineral density (BMC/BW in g/cm^2) was calculated (Hagaman et al., 1985).

After 24 hours fixation, the proximal third of each tibia was stained in Villanueva bone stain (Polysciences, Inc., Warrington, PA) for 4 days. The specimens were dehydrated by sequential changes of ascending concentrations of ethanol and acetone, and then embedded in methyl methacrylate (Eastman Organic Chemicals, Rochester, NY). Frontal sections (270 μm thick) of the proximal tibia were cut through the tibial eminence with a precision bone saw. Two sections from each tibia were ground to 100 μm thick and microradiographed on Kodak spectroscopic plates (649-0, Eastman Kodak, Rochester, NY; Miller and Jee, 1975). The 100 μm thick sections were mounted on plastic microscope slides with cyanoacrylate adhesive (910 Adhesive, Commercial Plastics, S.L.C., UT) and further ground to a thickness of 20 μm.

Microradiographs and a quantitative television microscope (QTM, Cambridge Instruments, Cambridge, England) coupled to a DEC 11/03 microcomputer were employed to measure metaphyseal tissue and hard tissue areas and perimeter. A 6 mm^2 area (2 mm wide × 3 mm long) of the secondary spongiosa was surveyed at 10× magnification (Smith and Jee, 1983; Jee and Smith, 1985). These measurements were used to calculate trabecular thickness, number, and separation according to Parfitt et al. (1983; Table 1).

Twenty micron thick sections and a digitizing image system were used to determine selected metaphyseal cancellous bone morphometry. The system consists of an epifluorescent microscope, a digitizing pad (Summagraphic, Fairfield, CT) coupled to an Apple MacIntosh SE computer and a morphometry program named "Stereology" (KSS Computer Engineers, Magna, UT). The metaphyseal area, trabecular area and perimeter, eroded surface, single- and double-labeled surface lengths, and interlabeling distance of double-fluorescent labels were measured in a 4.32 mm^2 area of secondary spongiosa at 125× magnification (Kimmel and Jee, 1980; Jee et al., 1983). Percent eroded and labeling surfaces, ratio of eroded to labeled surface, mineral apposition rate, and bone formation rate were calculated (Frost, 1977; Baron et al., 1984; Parfitt et al., 1987; Table 1).

The data from the overloaded versus age-matched control limbs were analyzed by the two-tailed Student *t* test.

RESULTS

Body and Soft Tissue Weights

Body weight of one-legged immobilized animals was reduced insignificantly (−6%) during the first 2 weeks, then remained constant thereafter, while that of control animals was unchanged throughout the experiment. No significant change was observed in soft tissue weights for either control or one-leg immobilized animals.

Although body weights were not significantly different between the one-legged immobilized animals and

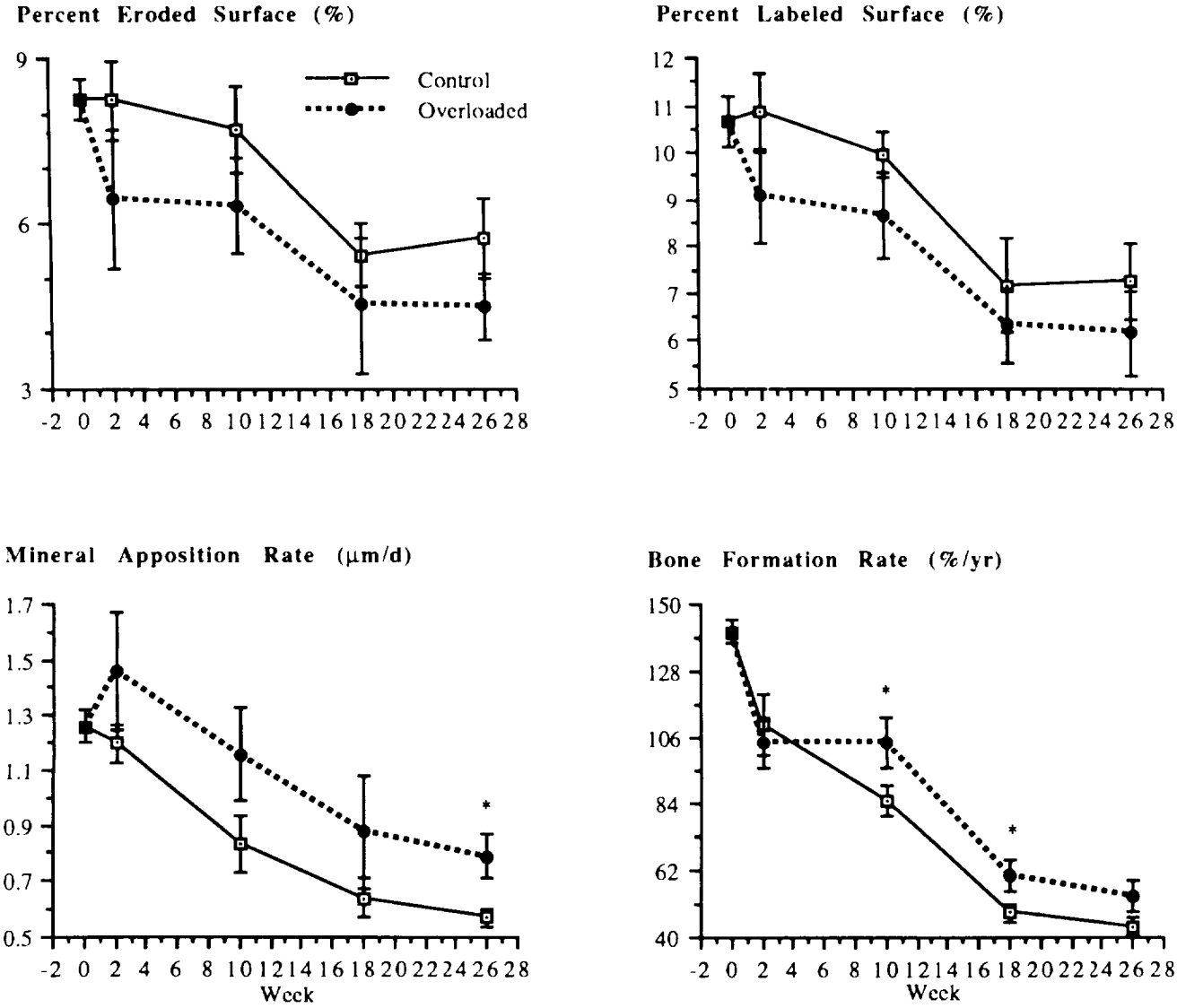

Fig. 5. The time course of cancellous bone histomorphometry changes of the proximal tibial metaphysis in controls (□) and overloaded (●) limbs. Y error bar represents standard error. The control animals show a progressive loss of eroded and labeled surfaces and diminishing bone apposition and bone formation rate with age. In overloaded tibial metaphyses, both percent eroded and labeled surfaces were insignificantly but consistently below the control levels. However, both mineral apposition and bone formation rates were consistently above the control levels. *$P < .05$.

the age-matched controls, the muscle weight was higher (+9%) on the overloaded legs than on the controls at 18 and 26 weeks of chronic overloading (Fig. 1).

Aging Bone Changes

In an earlier publication (Li et al., in press), age-related cancellous bone changes were characterized. Briefly, an insignificant decrease in trabecular bone mass and increase in trabecular thickness, a significant decrease in trabecular number, percent eroded surface, percent labeled surface, mineral apposition rate, and bone formation rate, and a significant increase in trabecular separation occurred in the aging cancellous bone (Tables 3, 4).

Skeletal Adaptive Responses

Bone mineral density increased significantly in both the proximal and distal femur: +6%, +6%, and +5% for the proximal and +9%, +7%, and +10% for the distal femur sites at 10, 18, and 26 weeks, respectively, of continuous overloading (Table 2; Fig. 2).

Significant morphometric changes were observed in the continuously overloaded proximal tibia. There was a significant increase in cancellous bone area of +41% and +47% with an accompanying increase of +31% and +32% in trabecular number and a decrease of −30% and −31% in trabecular separation after 18 and 26 weeks overloading. Mineral apposition rates were significantly elevated by +38% at 26 weeks, and the

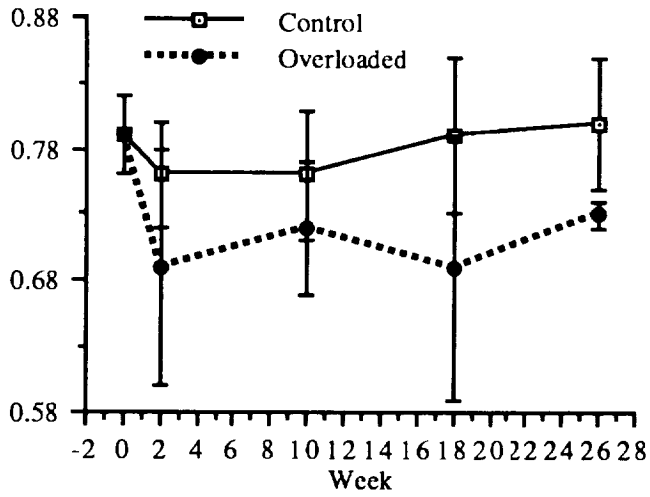

Fig. 6. The time course of the ratio of eroded to labeled surface of cancellous bone from the proximal tibial metaphysis of control (□) and overloaded (●) limbs. Y error bar represents standard error. Although the decreased ratio in the overloaded limb was not significant, this constant trend indicated that the decreasing rate was greater in eroded surface than in labeled surface.

bone formation rate increased by +23%, +26%, and +23% at 10, 18, and 26 weeks overloading compared to age-matched controls. More subtle, statistically insignificant changes occurred in percent eroded perimeter of −22%, −18%, −17%, and −22% and in percent labeled perimeter of −16%, −13%, −12%, and −15% at 2, 10, and 26 weeks overloading, respectively (Tables 3, 4; Figs. 3–7).

Table 4 compares the select static and dynamic histomorphometric changes in cancellous bone in the 15.5 month (26 weeks post-treatment) controls to that at 9 months and the same changes observed in 26 week overloaded cancellous bone to that of 0 and 26 week age-matched controls. Between 9 (0 week controls), and 15.5 months (26 week controls), trabecular bone area (−17%), and bone remodeling activities (% eroded surface − 31%, % labeled surface −32%, mineral apposition rate −55%, and bone formation rate −69%) were all reduced. The reduced cancellous bone lowered trabecular number (−22%) and increased trabecular separation (+33%) compared to 0 week controls.

When comparing the changes in the 26 week (15.5 months old) overloaded cancellous bone group to that in the 0 week (9 months old) control, trabecular area (+22%) and numbers (+18%) were increased and bone remodeling activities (% eroded surface −46%, % labeled surface −42%, mineral apposition rate −37%, and bone formation rate −63%) were depressed.

The comparison of the cancellous bone in the 26 week overloaded proximal tibiae to that in the 26 week (15.5 months old) controls offers a better picture of the impact of continuous overloading. There were dramatic changes in the trabecular area (+47%) accompanied by improved trabecular architecture (trabecular number, +32% and trabecular separation −31%). Bone remodeling activities were insignificantly depressed (% eroded surface −22% and % labeled surface −15%). More important was the stimulation of bone formation activities (mineral apposition rate +38% and bone formation rate +23%) that contributes to the positive bone balance.

DISCUSSION

It is well established that relatively strenuous exercise was necessary to increase muscle and bone mass (Watson, 1973; Jones et al., 1977; Montoye et al., 1980; Smith et al., 1981, 1984; Krolner et al., 1983; Holloszy and Coyle, 1984; Rose and Rothstein, 1982; Sinaki, 1988). Thus, it was not a surprise to detect that the increase in mechanical strain from hopping around on one limb was adequate to increase muscle and cancellous bone mass. We detected a +9% increase in muscle and a +41% increase in bone mass compared to age-matched controls at 18 and 26 weeks overloading. Further, a positive correlation between muscle and bone mass ($R = 0.56$) was also significantly ($P = 0.0001$) detected by linear regression analysis using combined data of control and overloaded limbs.

The cellular responses of overloading-induced positive bone balance included insignificant decreases in both eroded and labeled surfaces and significant increases in mineral apposition rate and bone formation rate, creating a positively accumulated bone bank (i.e., +41% and +47% at 18 and 26 weeks overloading). These findings suggest that the combination of decreased bone remodeling (i.e., reduced eroded and labeled surfaces), which reduced the remodeling space, and increased osteoblastic activity (i.e., increased mineral apposition and bone formation rates), which produced thicker trabecular, contributed to the increased bone mass. Increased osteoblastic activity can produce thicker trabecular packets by an imbalance of formation over resorption during bone remodeling and thicker trabecular by activating the bone formation phase of bone modeling (i.e., adding new bone without previous bone resorption; Fig. 7). Unfortunately, we were unable to measure trabecular packet thickness (i.e., mean wall thickness) in these 20 μm thick sections; therefore, we can not claim whether thicker trabecular packet contributed toward thicker trabeculae. However, we did observe increased bone formation (modeling) at the periosteal envelopes of overloaded tibial shafts in these animals, which will be the subject of an article in preparation on the response of cortical bone to overloading. Therefore, it is possible that in adult cancellous bone modeling was reactivated in these overloaded limbs. These observations and interpretations were in total agreement with Frost's suggestion on increased mechanical usage; modeling is stimulated and remodeling is depressed; thus, the stimulated modeling adds new cancellous bone, and the depressed remodeling reduces remodeling space and conserves spongiosa and corticoendosteal bone (Frost, 1986b, 1987, 1988a,b, in press).

The overload-induced changes in cancellous bone mass, as well as in the cellular mechanisms, appeared to be maximized at 18 weeks, but bone mass continued to climb slightly because bone apposition rate and bone formation rate remained elevated. Nevertheless, the changes in bone mass between 18 and 26 weeks is small, suggesting the proximal tibial metaphyseal cancellous bone has reached a new steady state of in-

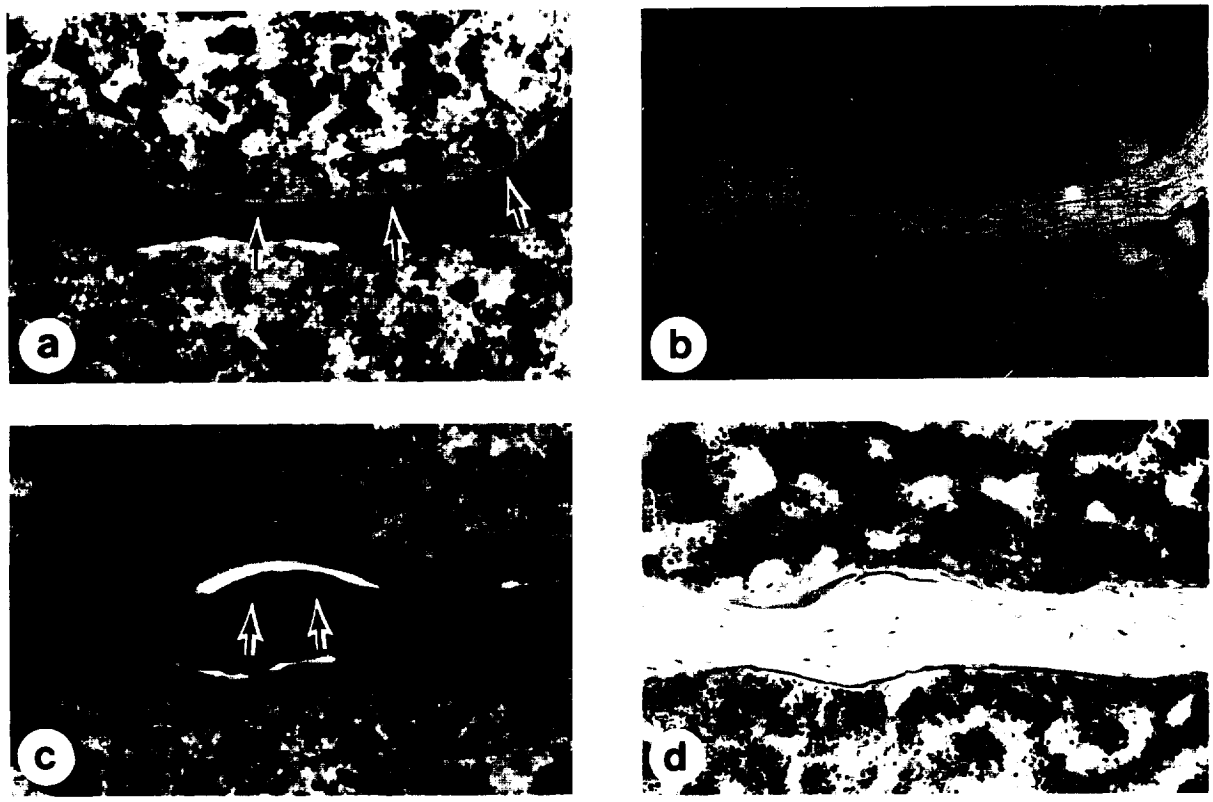

Fig. 7. Fluorescent and light microradiographs of proximal tibial metaphysis from control (**a,b**) and overloaded (**c,d**) rats. a: Double-fluorescent-labeled trabecula from a 9.5 month old control. c: Thickened trabecula after 2 weeks overloading with less labeled surface and greater interlabeling distance. This region of the trabeculum can be interpreted as a site of modeling in the formation mode (i.e., activation followed by formation). Matching light microphotographs are to the right (b,d). The tetracycline label given at 12 days (large arrows) and calcein label given at 2 days before sacrifice (small arrows). Twenty micron undecalcified section, Villanueva stained. ×500.

creased mass with lower turnover rate in a continued overloading environment.

Our study indicated that the adult skeleton can quickly adapt its cancellous bone mass to maintain the "optimal strain environment" of Rubin (1984; Rubin and Lanyon, 1984) or the "minimum effective strain set point" of Frost (1983, 1986a,b, 1988b), by a mechanism called the "mechanostat" by Frost (1987). More bone was deposited in overloaded bones owing to the increased skeletal strain beyond the optimal environment. The positive bone balance was achieved by depressing bone turnover and stimulating osteoblastic activity, which resulted in bone formation exceeding bone resorption during modeling and remodeling. The increased bone mass then acted in turn to reduce the increased functional strain back to the "optimal strain environment." Thus far, these observations are in agreement with Frost's three- and four-way rule for mechanical effects on lamellar bone modeling and remodeling, respectively (1988a, in press).

ACKNOWLEDGMENTS

The authors thank Dr. Yan L. Li and Rebecca B. Dell for their expert assistance and advice. The investigation was supported in part by research grants from NASA (NAG 2-435), Department of Energy and University of Utah (DEFG0289ER60764), National Institutes of Health (AR-38346), and Department of Energy (DE-AC02-76EV00119).

LITERATURE CITED

Baron R., R. Tross, and A. Vignery 1984 Evidence of sequential remodeling in rat trabecular bone: Morphology, dynamic histomorphometry, and changes during skeletal maturation. Anat. Rec., *208*:137–145.

Corwin, S.C. 1986 Wolff's law of trabecular architecture at remodeling equilibrium. J. Biomech. Eng., *108*:83–88.

Currey, J.D. 1984 The Mechanical Adaptations of Bones. Princeton University Press, Princeton, NJ.

Frost, H.M. 1964 The Laws of Bone Structure. Charles C. Thomas, Springfield, IL.

Frost, H.M. 1973 Bone Modeling and Skeletal Modeling Errors. Charles C. Thomas, Springfield, IL.

Frost, H.M. 1977 A method of analysis of trabecular bone dynamics. In: Bone Histomorphometry. P.O. Meunier, ed. Armour-Montagu, Paris, pp. 445–476.

Frost, H.M. 1983 The minimum effective strain: A determinant of bone architecture. Clin. Orthop., *175*:286–292.

Frost, H.M. 1986a Osteogenesis imperfecta. The set point proposal. Clin. Orthop., *216*:280–297.

Frost, H.M. 1986b Intermediary Organization of the Skeleton, Vols. I and II. CRC Press, Boca Raton, FL.

Frost, H.M. 1987 Bone "mass" and the "mechanostat": A proposal. Anat. Rec., *219*:1–9.

Frost, H.M. 1988a Structural adaptations to mechanical usage: A three-way rule for lamellar bone modeling. Comp. Vet. Orthop. Trauma, *1*:7–17, *2*:80–85.

Frost, H.M. 1988b Vital biomechanics: General concepts for structural adaptations to mechanical usage. Calcif. Tissue Int., *42*: 145–156.

Frost, H.M. Structural adaptations to mechanical usage: A four-way rule for lamellar bone remodeling. Anat. Rec., in press.

Hagaman, J.R., T.V. Sanchez, and R.C. Myers 1985 The effect of lactation on the mineral distribution profile of the rat femur by single photon absorptiometry. Bone, *6*:301–306.

Holloszy, J.O., and E.F. Coyle 1984 Adaptations of skeletal muscle to endurance exercise and their metabolic consequences. J. Appl. Physiol., *56*:831–838.

Jee, W.S.S., J. Inoue, K.W. Jee, and T. Haba 1983 Histomorphometric assay of the growing long bone. In: Handbook of Bone Morphology. H. Takahashi, ed., Nishimura Co., Ltd., Niigata City, Japan, pp. 101–122.

Jee, W.S.S., and J.M. Smith 1985 Image analysis of calcified tissue. In: Methods of Calcified Tissue Preparation. G.R. Dickson, ed. Elsevier, Amsterdam, pp. 673–696.

Jones, H.H., J.D. Priest, W.C. Hayes, C.C. Tichenor, and D.A. Nagel 1977 Humeral hypertrophy in response to exercise. J. Bone Joint Surg. [Am.], *59*:204–208.

Kimmel, D.B., and W.S.S. Jee 1980 A quantitative histologic analysis of the growing long bone metaphysis. Calcif. Tissue Int., *32*:113–122.

Krolner B., B. Toft, S.P. Nielsen, and E. Tondevold 1983 Physical exercise as prophylaxis against involutional vertebral bone loss: A controlled trial. Clin. Sci., *64*:541–546.

Li, X.J., W.S.S. Jee, S.Y. Chow, and D.M. Woodbury Adaptation of cancellous bone to aging and immobilization in the rat: A single photon absorptiometry and histomorphometry study. Anat. Rec., in press.

Lindgren, J.U. 1976a The effect of thyroparathyroidectomy on development of disuse osteoporosis in adult rats. Clin. Orthop., *118*: 251–255.

Lindgren, J.U. 1976b Studies of the calcium accretion rate of bone during immobilization in intact and thyroparathyroidectomized adult rats. Calcif. Tissue Res., *22*:41–47.

Lindgren, J.U., and S. Mattsson 1977 The reversibility of disuse osteoporosis. Calcif. Tissue Res., *23*:179–184.

Martin, R.B. 1973 The effects of geometric feedback in the development of osteoporosis. J. Biomech., *5*:447–455.

Mattsson, S. 1972 The reversibility of disuse osteoporosis. Acta Orthop. Scand. [Suppl.], *144*:1–135.

Miller, S.C., and W.S.S. Jee 1975 Ethane-1-hydroxyl, 1,1-diphosphonate (EHDP) effects on growth and modeling of the rat tibia. Calcif. Tissue Res., *18*:218–231.

Montoye, H.J., E.L. Smith, D.F. Fardon, and E.T. Howley 1980 Bone mineral in senior tennis players. Scand. J. Sports Sci., *2*:26–32.

Parfitt, A.M., M.K. Drezner, F.H. Glorieux, J.A. Kanis, H. Malluche, P.J. Meunier, S.M. Ott, and R.R. Recker 1987 Bone histomorphometry: Standardization of nomenclature, symbols, and units. J. Bone Min. Res., *2*:595–610.

Parfitt, A.M., C.H.E. Mathews, A.R. Villanueva, M. Kleerekoper, B. Frame, and D.S. Rao 1983 Relationship between surface, volume and thickness of iliac trabecular bone in aging and osteoporosis: Implications for the microanatomic and cellular mechanisms of bone loss. J. Clin. Invest., *72*:1396–1409.

Pauwels, F. 1980 Biomechanics of the Locomotor Apparatus. Springer-Verlag, Berlin.

Rose, S.J., and J.M. Rothstein 1982 Muscle mutability. Part I. General concepts and adaptations to altered patterns of use. Phys. Ther., *62*:1773–1782.

Roux, W. 1895 Gesammelte Abhandlunger uber Entwicklungsmechanik der Organismen. Vol I and II. W. Englemann, Leipzig.

Rubin, C.T. 1984 Skeletal strain and the functional significance of bone architecture. Calcif. Tissue Int., *365*:511–518.

Rubin, C.T., and L.E. Lanyon 1984 Regulation of bone formation by applied dynamic loads. J. Bone Joint Surg. [Am.], *66*:397–402.

Saville, P.D., and M.P. Whyte 1969 Muscle and bone hypertrophy. Postive effect of running exercise in the rat. Clin. Orthop., *65*: 81–88.

Sevastikoglou, J.A., and S. Mattsson 1976 Changes in composition and metabolic activity of the skeletal parts of the extremity of the adult rat following immobilization in a plaster cast. Acta Chir. Scand. [Suppl.], *467*:21–25.

Sinaki, M. 1988 Exercise and physical therapy. In: Osteoporosis, Diagnosis and Management. B.L. Riggs and L.J. Melton, eds., Raven Press, New York, pp. 457–479.

Smith, E.L., and C. Gilligan 1989 Mechanical forces and bone. In: Bone and Min. Res., W.A. Peck, ed. Elsevier, New York, vol. 6, pp. 139–173.

Smith J.M., and W.S.S. Jee 1983 Automated bone histomorphometry. In: Bone Histomorphometry: Techniques and Interpretation. R.R. Recker, ed. CRC Press, Inc., Boca Raton, FL, pp. 285–296.

Smith, E.L., W. Reddan, and P.E. Smith 1981 Physical activity and calcium modalities for bone mineral increase in aged women. Med. Sci. Sports Exerc., *13*:60–64.

Smith, E.L., P.E. Smith, Ensign C.J., and M.M. Shea 1984 Bone involution decrease in exercising middle-aged women. Calcif. Tissue Int., *36*:S129–S138.

Thomaidis, V.T., and T.S. Lindholm 1976 The effect of remobilization on the extremity of the adult rat after short-term immobilization in a plaster cast. Acta Chir. Scand. [Suppl.], *467*:36–39.

Uhthoff, H.K., and Z.F.G. Jaworski 1978 Bone loss in response to long-term immobilization J. Bone Joint Surg. [Br.], *60*:420–429.

Uhthoff, H.K., G. Sekaly, and Z.F.G. Jaworski 1985 Effect of long-term non-traumatic immobilization on metaphyseal spongiosa in young adult and old beagle dogs. Clin. Orthop., *192*:278–283.

Watson, R.C. 1973 Bone growth and physical activity. In: International Conference on Bone Mineral Measurements. R.B. Mazess, ed. DHEW Publication No. NIH 75-683, Washington, DC, pp..

Wolff, J. 1892 Das Gasetz der Transformation der Knochen. Hirschwald, Berlin.